JOURNAL OF GUIDANCE, CONTROL, AND DYNAMICS
Vol. 40, No. 3, March 2017

Engineering Notes

Detumbling Space Debris Using Modified Yo-Yo Mechanism

Vadim Yudintsev* and Vladimir Aslanov†
Samara National Research University, 443086, Samara, Russia

DOI: 10.2514/1.G000686

Nomenclature

$\boldsymbol{A}_d$	=	matrix that transforms coordinates from $Dx_dy_dz_d$ to $Cxyz$ frame
d	=	diameter of the reel, m
J_x, J_y, J_z	=	moments of inertia of the target, kg · m^2
$\boldsymbol{K}$	=	angular momentum vector of the target, (kg · m^2)/s
l_i	=	unwrapped length of ith wire, m
$l_{\max}$	=	length of ith wire, m
m	=	mass of the target, kg
m_i	=	mass of the ith mass, kg
$\boldsymbol{q}$	=	vector of the generalized coordinates
$\boldsymbol{r}_i$	=	position vector of ith mass, m
$\boldsymbol{T}_i$	=	tension of ith wire, N
$\boldsymbol{v}_i$	=	velocity vector of ith mass, m/s
x, y, z	=	target coordinates, m
$\alpha_i, \beta_i, \gamma_i$	=	angles describing position of ith yo-yo mass, rad
ϑ	=	angle between longitudinal axis of the target and the tether, rad
$\boldsymbol{\rho}_d$	=	position vector of $Dx_dy_dz_d$ reference frame, m
ψ, θ, φ	=	Euler angles describing orientation of the target, rad

I. Introduction

IN THIS note, we consider a method for detumbling a space debris object using a modified yo-yo mechanism that does not contribute to space debris. A mathematical model of the spatial motion of the space debris object with attached yo-yo mechanism is developed. Several numerical examples demonstrate the possibility of using the proposed scheme to despin space debris.

Large objects like orbital stages, boosters, and nonfunctional spacecraft are potential sources of orbital debris. Recent spacecraft and orbital stages respect the postmission disposal at their end of life, but objects launched many years ago pose serious hazard to active satellites. To reduce this risk, large objects like old orbital stages should be removed from the most used orbits [1]. The last few years, several methods of active debris removal (ADR) are proposed [2–7]. Some of these methods employ using a tethered space tug for rendezvous, docking, and towing dangerous objects to a disposal orbit or into the atmosphere for burn up [8–11]. The ADR mission can be planned as a hosted payload mission. For example, the upper stage after the deployment of the main payload can be used as a space tug to deorbit space debris. In this case, the upper stage can carry an autonomous module (ADR module), which performs ADR-specific tasks after the separation of the main payload. These tasks include the final approach, docking, and detumbling space debris (target) [12]. The ability to capture and safely deorbit depends on the attitude motion of the debris. The attitude motion of a nonfunctional satellite is determined by the performance of its control systems at the end of life. Orbital stages are not controlled after the separation of payload, and so the attitude motion is determined by the work of the payload separation devices. Upper stages after the separation of the payload can start rotating around the longitudinal axis due to the redistribution of the angular momentum between the body of orbital stage and the rotating parts of the thruster (e.g., elements of pump).

Detumbling can be performed before docking with the target using, for example, a brush-type contactor as the end effector of a robot arm [2,13] or repeated mechanical impulses [14]. The attitude motion of the ADR module can be synchronized to the target's so that the capturing operation can be conducted with small relative motion [15]. A probe–cone mechanism can be used for the docking with the tumbling target using the nozzle of the target as a "cone" part of the probe–cone mechanism [16,17]. For safe docking of the ADR module and docked debris with the space tug, the space debris should be detumbled. Several techniques can be used to do this. For example, energy dissipation can be used to change the motion of the debris [18]. The docking module can be equipped with rocket thrusters. The attitude motion of the target can be partially stabilized by using the tether, which connects the ADR module and the space tug [19–21]. The general rotational motion of space debris involves spin, nutation, and precession. If the tether attachment point is on the longitudinal axis of the debris, the spin rate around this axis cannot be eliminated using the tether.

Here, we propose to use a modified yo-yo mechanism to despin a space debris object. We assume that the ADR module docked with the target debris (the docking process with tumbling debris is a separate complex task, which is beyond the scope of this note). We imagine the following mission scenario using the modified yo-yo mechanism (Fig. 1). The yo-yo mechanism can be installed on the ADR module. During the final approach stage, the ADR module is separated from the tug and docks with target using, for example, a probe–cone mechanism [16] (Fig. 1a). At the next stage, the target is despinned using a modified yo-yo mechanism, which does not contribute to space debris (Fig. 1b). The transverse angular velocity of the target can be eliminated using the tether (Fig. 1c). After the detumbling, the ADM module with the target debris can be docked to the tug (Fig. 1c), or alternatively, the space tug can start deorbit burn to remove the tethered debris from the orbit [8,11,22–24].

The article is organized as follows. Section II describes the modified yo-yo mechanism. Section III presents mathematical model of the spatial motion of the yo-yo mechanism. Section IV shows several numerical examples that illustrate the possibility of using the yo-yo mechanism to despin tumbling space debris. This work continues a series of studies [10,11] where the postburn phase of ADR is considered.

II. Modified Yo-Yo Mechanism

The well-known yo-yo mechanism has two wires with masses on the ends. The wires are wrapped around the reel, and the masses are secured by a release mechanism. At a preselected time, the masses are released and "take" the momentum of the body (satellite or rocket) so that the spin of the body is reduced [25,26]. In a traditional yo-yo scheme, it is expected that the wires are released from the satellite after the wire will take radial position. Obviously, in an ADR mission,

Received 29 May 2016; revision received 19 July 2016; accepted for publication 9 September 2016; published online 11 January 2017.

*Associate Professor, Theoretical Mechanics Department, 34 Moskovskoye Shosse.

†Head, Theoretical Mechanics Department, 34 Moskovskoye Shosse.

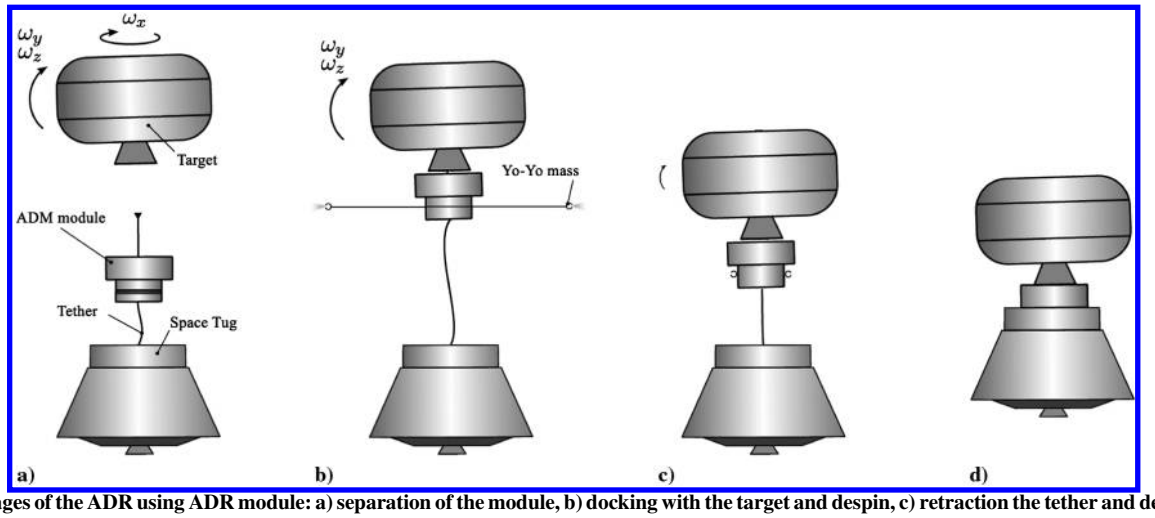

Fig. 1 Stages of the ADR using ADR module: a) separation of the module, b) docking with the target and despin, c) retraction the tether and detumbling, and d) docking with the tug.

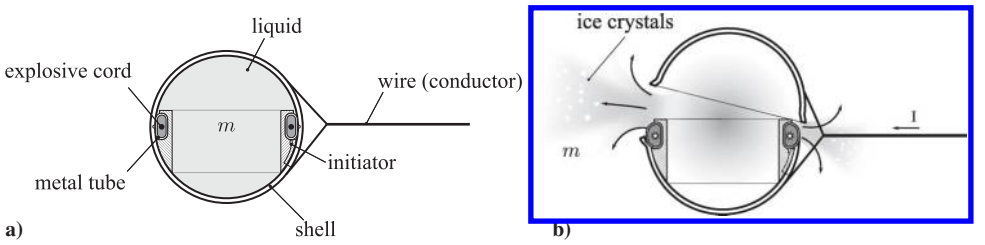

Fig. 2 Modified yo-yo mass.

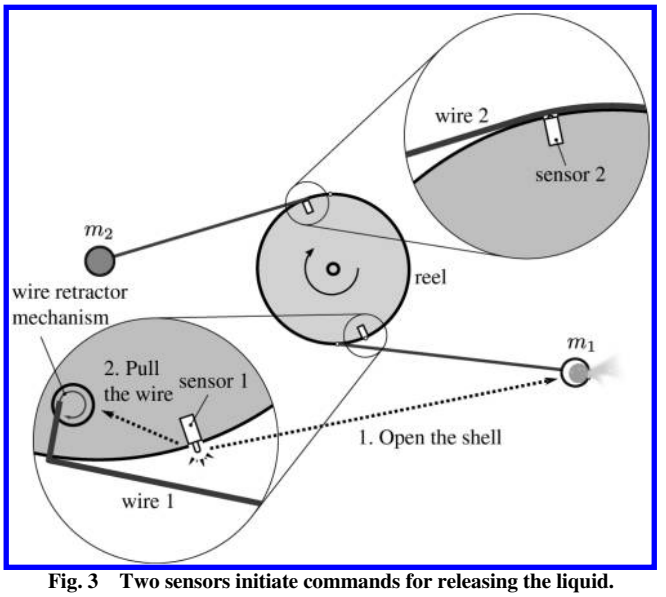

Fig. 3 Two sensors initiate commands for releasing the liquid.

this algorithm is not allowed. The hardware used in an ADR mission should not contribute to the space debris.

To prevent contributing additional debris during ADR, we propose to use modified masses attached to the wires. Each mass is a shell filled with a liquid. It can be water or any liquid with a low freezing point (e.g., a solution of alcohol) to prevent freezing the liquid during the flight. Instead of releasing the whole mass, the shell opens at the end of the despin process so that the liquid evaporates quickly, turning into ice crystals.

The wire to which the mass is attached can be used as a conductor that transfers signal for opening the shell and releasing the liquid (Fig. 2). The separation of the two parts of the shell can be performed by using the well-known Super*Zip separation device broadly used in space applications (Fig. 2, U.S. patent 3698281, [27–29]).

The liquid from ith mass should be released when the ith wire reaches radial position. At that point in time, the angular velocity of the target around its longitudinal axis is close to zero, and so an angular velocity sensor can be used to initiate the process of releasing the liquid from the shells. Also, the signal for releasing the liquid can be initiated by a simple sensing device (e.g., microswitch), which indicates that the wire has unwound from the reel (Fig. 3).

The sensor can be placed near the wire attachment point. The sensor, when the wire reaches it, energizes the Super*Zip separation device after some delay to account for the motion of the wire from the tangent to radial position. The sensor can also energize a wire retractor mechanism (in the form of a spring loaded reel). The wire retractor mechanism pulls the wire to get back the empty shell to prevent the wires from twisting and tangling around the ADR module (Fig. 3).

The attitude motion of the debris induces out-of-plane motion of the wires. This motion can cause the wires to come off the reel due to its motion with the target. To prevent this, the reel can be equipped with a device that constrains the motion of the wires. Figure 4 demonstrates one possible example of such a device.

The motion of each wire can be guided by a light slider (wire guide), which is moved in the circle of the reel radius 4. The slider prevents the wires from coming off the reel but does not inhibit the motion of the wires in the plane of the reel. The necessity of this device is questionable and should be tested experimentally.

III. Mathematical Model

The yo-yo theme has already been discussed in the literature [25,26,30,31], but the traditional scheme assumes that the body that needs to be despinned rotates around one of its axis. The rotational motion of space debris involves spin, nutation, and precession. In this case, we need to build a mathematical model of the spatial motion of the wires with the masses that takes into account the attitude motion of the debris.

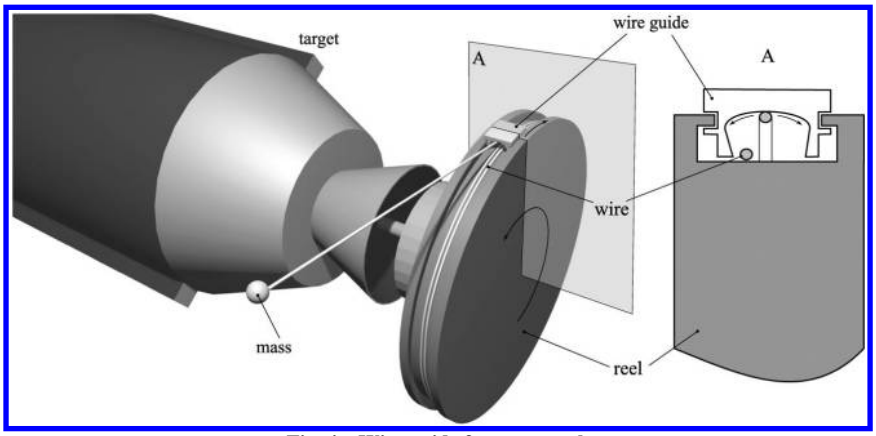

Fig. 4 Wire guide for yo-yo reel.

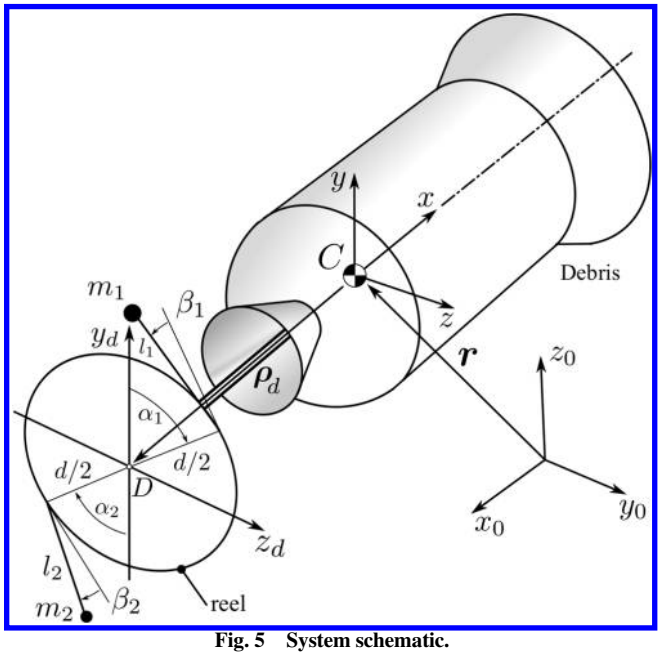

Fig. 5 System schematic.

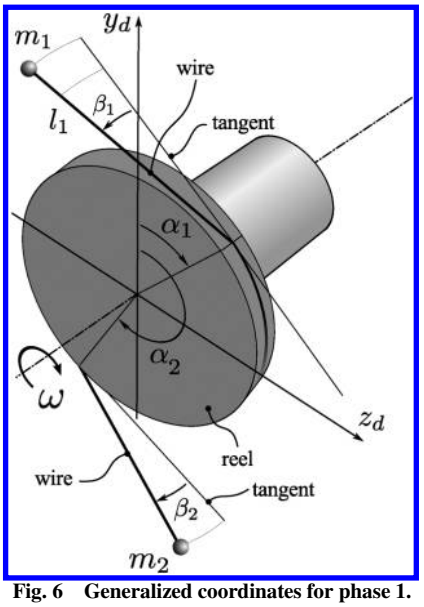

Fig. 6 Generalized coordinates for phase 1.

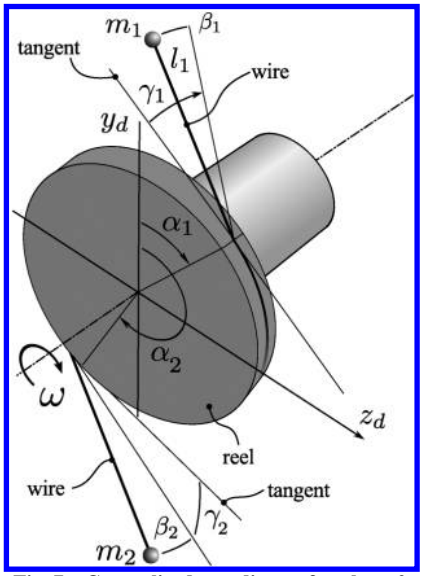

Fig. 7 Generalized coordinates for phase 2.

A. System Description

The scheme of the considered system is shown in Fig. 5. This mechanical system consists of three bodies: space debris (target) with docked ADM module equipped with the reel and two wires with masses m_1 and m_2. The target is considered as a rigid body, and two masses are considered as point masses. The motion of the system is considered relative to the inertial frame $Ox_0y_0z_0$. External forces (gravitational, magnetic, etc.) are neglected.

The motion of each wire with the mass can be divided into two phases [25]. In phase 1, the wire is changing in length and is tangent to the reel (Fig. 6). During phase 2, the length of the wire is constant. The wire rotates around its attachment point (Fig. 7). Because of the attitude motion of the debris, the unwrapping of the wires can be nonsynchronous so that the wires can be in different phases of motion. This aspect should be taken into consideration.

In the next section, the kinematics of the spatial yo-yo system is described. The position and velocity vectors of the masses are obtained for each phase of the motion.

B. Kinematic of the System

The configuration of the system in phase 1 is described by 10 coordinates:

$$\boldsymbol{q} = (x, y, z, \psi, \theta, \varphi, \alpha_1, \beta_1, \alpha_2, \beta_2) \tag{1}$$

where x, y, z are the coordinates of the center of mass of the debris in frame $Ox_0y_0z_0$; and ψ, θ, and φ are the Euler angles (3-1-3), which

describe the orientation of the debris relative to the $Ox_0y_0z_0$ frame [32]. The last four coordinates in Eq. (1) describe the positions of the wires. Angles α_1, β_1 and α_2, β_2 describe the positions of the yo-yo masses relative to the local reference frame $Dx_dy_dz_d$ fixed to the target. The origin of the reference frame $Dx_dy_dz_d$ is located in the plane of the reel and is given by the vector $\boldsymbol{\rho}_d$. The plane of the reel coincides with the plane Dy_dz_d. It is assumed that the wires are wrapped around the reel in the plane Dy_dz_d and do not affect each other (Fig. 5).

The position of the ith mass relative to the reference frame $Dx_dy_dz_d$ is given by the vector $\boldsymbol{\rho}_i$, which is parameterized by a different set of angles depending on the phase of the motion. In phase 1, vector $\boldsymbol{\rho}_i$ depends on the angles α_i, β_i (Fig. 6):

$$\boldsymbol{\rho}_i = \begin{bmatrix} -l_i \sin\beta_i \\ l_i \cos\beta_i \sin\alpha_i + d/2 \cos\alpha_i \\ d/2 \sin\alpha_i - l_i \cos\beta_i \cos\alpha_i \end{bmatrix} \tag{2}$$

The relative velocity of the ith mass is given by

$$\dot{\boldsymbol{\rho}}_i = \frac{d}{2}\begin{bmatrix} -\sin\beta_i \\ (2l_i \cos\alpha_i/d + \sin\alpha_i)\cos\beta_i - \sin\alpha_i \\ (2l_i \sin\alpha_i/d - \cos\alpha_i)\cos\beta_i + \cos\alpha_i \end{bmatrix}\dot{\alpha}_i + l_i\begin{bmatrix} -\cos\beta_i \\ -\sin\beta_i \sin\alpha_i \\ \sin\beta_i \cos\alpha_i \end{bmatrix}\dot{\beta}_i \tag{3}$$

In phase 1, the length of ith wire unwound is

$$l_i = (\alpha_i - \alpha_{i0})d/2 \tag{4}$$

where $\alpha_{10} = 0$ and $\alpha_{20} = \pi$; d is the diameter of the reel.

In phase 2, the position of the ith mass is described by two angles β_i and γ_i, which represent the orientation of the wire relative to the tangent plane of the reel that is passed through the wire attachment point (Fig. 7). In phase 2, the vector $\boldsymbol{\rho}_i$ depends on the angles γ_i, β_i and constant angle $\alpha_i = \alpha_{\text{ie}}$:

$$\boldsymbol{\rho}_i = \begin{bmatrix} -l_i \sin\beta_i \\ d/2 \cos\alpha_i + l_i \cos\beta_i \sin(\alpha_i + \gamma_i) \\ d/2 \sin\alpha_i - l_i \cos\beta_i \cos(\alpha_i + \gamma_i) \end{bmatrix} \tag{5}$$

The relative velocity of the ith mass for phase 2 is

$$\dot{\boldsymbol{\rho}}_i = l_i\begin{bmatrix} 0 \\ \cos\beta_i \cos(\alpha_i + \gamma_i) \\ \cos\beta_i \sin(\alpha_i + \gamma_i) \end{bmatrix}\dot{\gamma}_i + l_i\begin{bmatrix} \cos\beta_i \\ -\sin\beta_i \sin(\alpha_i + \gamma_i) \\ \sin\beta_i \cos(\alpha_i + \gamma_i) \end{bmatrix}\dot{\beta}_i \tag{6}$$

The length of the ith wire during phase 2 remains constant:

$$l_i = (\alpha_{ie} - \alpha_{i0})d/2 \tag{7}$$

where α_{ie} is the final value of the angle α_i in phase 1.

Now, the position of the ith yo-yo mass relative to the frame $Ox_0y_0z_0$ can be written as follows:

$$\boldsymbol{r}_i = \boldsymbol{r} + \boldsymbol{A}(\boldsymbol{\rho}_d + \boldsymbol{A}_d\boldsymbol{\rho}_i), \qquad i = 1, 2 \tag{8}$$

where $\boldsymbol{r} = (x, y, z)^T$, and $\boldsymbol{A}$ is the matrix that transforms the coordinates from the body frame $Cxyz$ to the frame $Ox_0y_0z_0$. Matrix $\boldsymbol{A}$ depends on the angles ψ, θ, and φ [32]:

$$\boldsymbol{A} = \begin{bmatrix} c_\varphi c_\psi - c_\theta s_\varphi s_\psi & -c_\psi s_\varphi - c_\theta c_\varphi s_\psi & s_\theta s_\psi \\ c_\theta c_\psi s_\varphi + c_\varphi s_\psi & c_\theta c_\varphi c_\psi - s_\varphi s_\psi & -c_\psi s_\theta \\ s_\theta s_\varphi & c_\varphi s_\theta & c_\theta \end{bmatrix} \tag{9}$$

where $c_f = \cos f$, $s_f = \sin f$, $f = \psi,\ \theta,\ \varphi$, and $\boldsymbol{A}_d$ is the transformation matrix that transforms coordinates from the frame $Dx_dy_dz_d$ to the frame $Cxyz$. If the frame $Dx_dy_dz_d$ is shifted relative to the body frame $Cxyz$ along the Cx axis, then the matrix $\boldsymbol{A}_d$ is an identity matrix $\boldsymbol{A}_d = \boldsymbol{E}$.

C. Motion Equations

The Lagrangian formalism is used to derive the equations of the motion:

$$\frac{\mathrm{d}}{\mathrm{d}t}\frac{\partial T}{\partial \dot{q}_i} - \frac{\partial T}{\partial q_i} = 0, \qquad i = 1, \ldots, n \tag{10}$$

where $q_i, i = 1, \ldots, n$ are generalized coordinates. The kinetic energy T of the system has the form

$$2T = m\boldsymbol{v}^2 + \boldsymbol{\omega}^T\boldsymbol{J}\boldsymbol{\omega} + m_1\boldsymbol{v}_1^2 + m_2\boldsymbol{v}_2^2 \tag{11}$$

where m is the mass of the target with the ADR module; $\boldsymbol{J} = \mathrm{diag}(J_x, J_y, J_z)$ is the inertia tensor of the target; $\boldsymbol{v} = \dot{\boldsymbol{r}} = (\dot{x}, \dot{y}, \dot{z})^T$ is the velocity of the target; $\boldsymbol{\omega}$ is the angular velocity vector of the target; and $\boldsymbol{v}_i$ is the velocity of the ith yo-yo mass:

$$\boldsymbol{v}_i = \frac{\mathrm{d}\boldsymbol{r}_i}{\mathrm{d}t} = \boldsymbol{v} + \boldsymbol{A}\tilde{\boldsymbol{\omega}}(\boldsymbol{\rho}_d + \boldsymbol{A}_d\boldsymbol{\rho}_i) + \boldsymbol{A}\boldsymbol{A}_d\dot{\boldsymbol{\rho}}_i, \qquad i = 1, 2 \tag{12}$$

$\tilde{\boldsymbol{\omega}}$ is a skew-symmetric matrix:

$$\tilde{\boldsymbol{\omega}} = \begin{bmatrix} 0 & -\omega_z & \omega_y \\ \omega_z & 0 & -\omega_x \\ -\omega_y & \omega_x & 0 \end{bmatrix} \tag{13}$$

The angular velocity of the target is parameterized by the derivatives of the Euler angles ψ, θ, φ:

$$\boldsymbol{\omega} = \begin{bmatrix} \sin\theta\sin\varphi & \cos\varphi & 0 \\ \sin\theta\cos\varphi & -\sin\varphi & 0 \\ \cos\theta & 0 & 1 \end{bmatrix}\begin{bmatrix} \dot{\psi} \\ \dot{\theta} \\ \dot{\varphi} \end{bmatrix} \tag{14}$$

Substituting Eqs. (3), (12), (14), and (10), we obtain the equations of the system for phases 1 and 2. The equations obtained are very cumbersome and are not presented here. One can use mathematical software system to get these equations. We used Wolfram Mathematica for this purpose.

The wire length needed to reduce the angular velocity of the rotating object from ω_0 to zero does not depend on the initial angular velocity and is given by the expression [30]

$$l_{\max} = \sqrt{\frac{J_x}{2m_i}} - d/2 \tag{15}$$

D. Initial Conditions

The initial conditions for phase 1 are

$$x(0) = y(0) = z(0) = \psi(0) = \theta(0) = \varphi(0) = 0$$
$$\alpha_1(0) = \alpha_2(0) = \beta_1(0) = \beta_2(0) = 0$$
$$\dot{x}(0) = \dot{y}(0) = \dot{z}(0) = 0$$
$$\dot{\psi}(0) = \dot{\psi}_0, \quad \dot{\theta}(0) = \dot{\theta}_0, \quad \dot{\varphi}(0) = \dot{\varphi}_0$$
$$\dot{\alpha}_1(0) = \dot{\alpha}_2(0) = \dot{\beta}_1(0) = \dot{\beta}_2(0) = 0$$

where $\dot{\psi}_0$, $\dot{\theta}_0$, and $\dot{\varphi}_0$ are initial values for Euler angle derivatives, which depend on the angular velocity of the target [Eq. (14)]. The integration process for phase 1 continues until the length of the unwrapped wire is less than $l_{\max}$:

$$l_i < l_{\max}, \qquad i = 1, 2 \tag{16}$$

If, for example, l_1 reaches $l_{\max}$ at $t = t_1$ and $l_2(t_1)$ is less than $l_{\max}$, then Eq. (10) should be built using expression (6) for $\dot{\boldsymbol{\rho}}_1$ and Eq. (3) for $\dot{\boldsymbol{\rho}}_2$. The generalized coordinates for this phase are

$$q = (x, y, z, \psi, \theta, \varphi, \gamma_1, \beta_1, \alpha_2, \beta_2) \tag{17}$$

.

The initial conditions for the new variable γ_1 are

$$\gamma_1(t_1) = 0, \qquad \dot{\gamma}_1(t_1) = \dot{\alpha}_1(t_1) \tag{18}$$

The next phase starts when the length of the second wire reaches $l_{\max}$. Assume that this happened at $t = t_2$. The equations [Eq. (10)] for the next phase should be built using expression (6) for $\dot{\boldsymbol{\rho}}_1$ and $\dot{\boldsymbol{\rho}}_2$. The generalized coordinates for this phase are

$$q = (x, y, z, \psi, \theta, \varphi, \gamma_1, \beta_1, \gamma_2, \beta_2) \tag{19}$$

and the initial conditions for the new variable γ_2 are

$$\gamma_2(t_2) = 0, \qquad \dot{\gamma}_2(t_2) = \dot{\alpha}_2(t_2) \tag{20}$$

The integration process for this phase continues until

$$\gamma_1 < \pi/2 \quad \text{and} \quad \gamma_2 < \pi/2 \tag{21}$$

In the classical yo-yo scheme, the wire should be detached from the reel when the wire reaches the radial position relative to the reel. If, for example, γ_1 reaches $\pi/2$ at $t = t_3$, then we should exclude the first mass from the model and build a new Eq. (10) for the following generalized coordinates:

$$q = (x, y, z, \psi, \theta, \varphi, \gamma_2, \beta_2) \tag{22}$$

The initial conditions for the coordinates [Eq. (22)] are copied from the previous phase.

E. Wire Tension

Because of the attitude motion of the debris, it is possible that the wires could become slack. The lack of tension of the wire makes the motion of the mass unpredictable and can cause premature release of the liquid from the mass. We should follow the tensions of the wires to make sure that the tension does not fall to zero.

The tension $\boldsymbol{T}_i$ of the ith wire can be obtained from the obvious equation of the ith mass:

$$m_i \ddot{\boldsymbol{r}}_i = \boldsymbol{T}_i \tag{23}$$

where $\ddot{\boldsymbol{r}}_i$ is the absolute acceleration of the ith mass that can be found by differentiating expression (12):

$$\ddot{\boldsymbol{r}}_i = \frac{\mathrm{d}\boldsymbol{v}_i}{\mathrm{d}t} = \ddot{\boldsymbol{r}} + \boldsymbol{A}\tilde{\boldsymbol{\omega}}\,\tilde{\boldsymbol{\omega}}(\boldsymbol{\rho}_d + \boldsymbol{A}_d\boldsymbol{\rho}_i) + \boldsymbol{A}\tilde{\boldsymbol{\varepsilon}}(\boldsymbol{\rho}_d + \boldsymbol{A}_d\boldsymbol{\rho}_i) + 2\boldsymbol{A}\tilde{\boldsymbol{\omega}}\boldsymbol{A}_d\dot{\boldsymbol{\rho}}_i + \boldsymbol{A}\boldsymbol{A}_d\ddot{\boldsymbol{\rho}}_i, \qquad i = 1, 2 \tag{24}$$

where $\tilde{\boldsymbol{\varepsilon}}$ is an angular acceleration matrix of the target:

$$\tilde{\boldsymbol{\varepsilon}} = \begin{bmatrix} 0 & -\varepsilon_z & \varepsilon_y \\ \varepsilon_z & 0 & -\varepsilon_x \\ -\varepsilon_y & \varepsilon_x & 0 \end{bmatrix} \tag{25}$$

The ith wire is tensioned if the tension vector $\boldsymbol{T}_i$ directed toward ith wire contact point on the reel

$$T_i = -m_i \ddot{\boldsymbol{r}}_i \cdot \boldsymbol{\tau}_i > 0 \tag{26}$$

where $\boldsymbol{\tau}_i$ is the unit vector parallel to ith wire:

$$\boldsymbol{\tau}_i = \frac{\boldsymbol{A}\boldsymbol{\rho}_i}{|\boldsymbol{A}\boldsymbol{\rho}_i|} \tag{27}$$

IV. Simulation Results

The purpose of this section is to investigate the motions of the yo-yo masses during the despin process while the target undergoes complex attitude motion.

Let us consider the detumbling process of an oblate target. The target is an axisymmetric orbital stage with mass of a 1000 kg, and the inertia tensor $\boldsymbol{J} = \mathrm{diag}(2000, 1000, 1000)\mathrm{kg} \cdot \mathrm{m}^2$. The yo-yo reel is fixed at a distance of 4 m along the longitudinal axis from the target's center of mass. The parameters of the system are presented in Table 1. The length of the yo-yo wire for the masses $m = m_1 = m_2 = 6.5$ kg should be equal to Eq. (15):

$$l_{\max} = \sqrt{\frac{J_x}{2\ \mathrm{m}}} = d/2 = \sqrt{\frac{1300\ \mathrm{kg} \cdot \mathrm{m}^2}{2 \cdot 6.5\ \mathrm{kg}}} - 1\ \mathrm{m} = 9\ \mathrm{m}$$

Three cases are considered, which differ from each other by the nutation angle ϑ between the angular momentum vector $\boldsymbol{K} = \boldsymbol{J} \cdot \boldsymbol{\omega}$ of the target and the axis of symmetry of the target Cx (Table 2):

$$\vartheta = \arccos\frac{J_x\omega_{x0}}{|\boldsymbol{J} \cdot \boldsymbol{\omega}|} \tag{28}$$

In the first case, the target rotates around longitudinal axis Cx with the rate $\omega_{x0} = 0.6$ rad/s, and the nutation angle ϑ between the longitudinal axis and angular momentum vector $\boldsymbol{K}$ is small.

In the second case, the nutation angle of the target is equal to 4 deg, which corresponds to the angular rate around the Cz axis of about 0.05 rad/s. In the third case, the nutation angle of the target is equal to 11 deg, and so the angular rate around the Cz axis is about 0.15 rad/s.

The differential equations are integrated using a built-in Wolfram Mathematica function "NDSolve".

A. Case 1

The first case demonstrates the classical yo-yo scheme. In this case, the target rotates around its axis of symmetry, and the masses move near the plane of the reel Dy_dz_d. The simulation results are shown in Fig. 8.

At approximately 15 s after starting the despin process, the wires are unwound, and 2 s later, the wires reach the radial position.

Table 1 Parameters of the system

Parameter	Value	Parameter	Value	Parameter	Value
m	1000 kg	m_1	6.5 kg	m_2	6.5 kg
J_x	1500 kg · m^2	J_y	1000 kg · m^2	J_z	1000 kg · m^2
ρ_x	−4 m	ρ_y	0 m	ρ_z	0 m
d	2 m	— —	— —	— —	— —

Table 2 Simulation cases

Case	ω_{0x}, rad/s	ω_{0z}, rad/s	ϑ, deg
1	0.6	0.01	1
2	0.6	0.05	4
3	0.6	0.15	11

Figure 8a shows the projections of the angular velocity vector of the target on its Cx, Cy, and Cz axes. We can see a reduction in the projection of the angular velocity in the Cx axis from 0.6 rad/s to zero within 17 s. Figure 8b shows the time history of the angular momentum $|\boldsymbol{K}|$. The angular momentum also reaches zero at time $t = 17$ s. Figure 8c shows the time history of the angles β_1 and β_2. The inclination of each wire to the reel plane Dy_dz_d is small. Figure 8d shows the time history of the wires' tension. The tensions of the wires are close to each other and greater than zero.

B. Case 2

In the second case, the Cx axis of the target is precessed around the angular momentum vector $\boldsymbol{K}$ with a nutation angle of 4 deg.

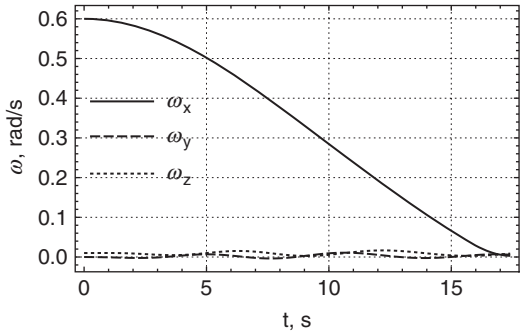

a) Angular velocity

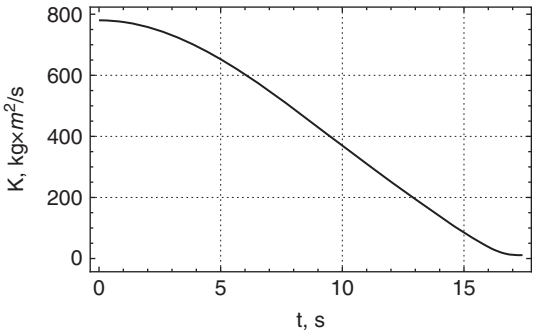

b) Angular momentum

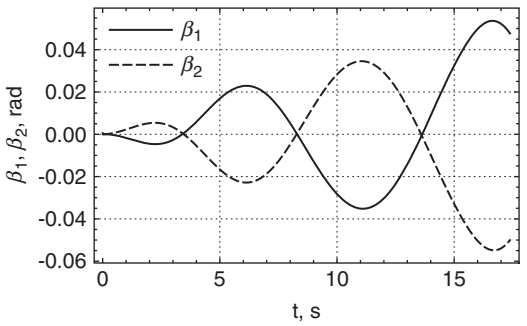

c) Angles β_1, β_2

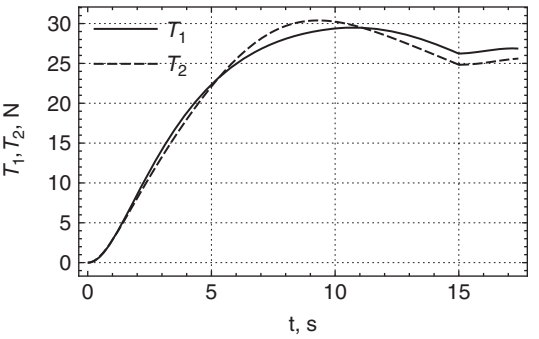

d) Tensions T_1, T_2

Fig. 8 Simulation results for case 1.

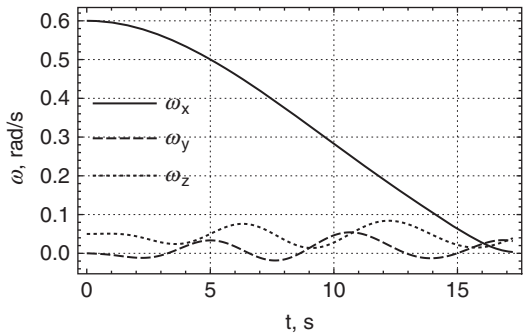

a) Angular velocity

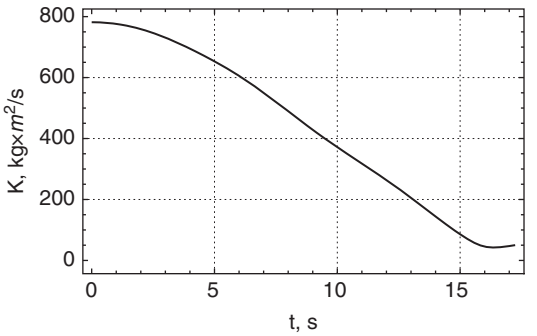

b) Angular momentum

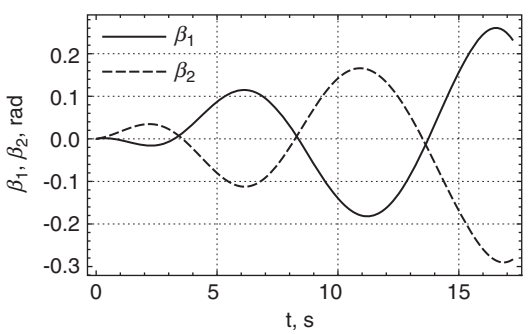

c) Angles β_1, β_2

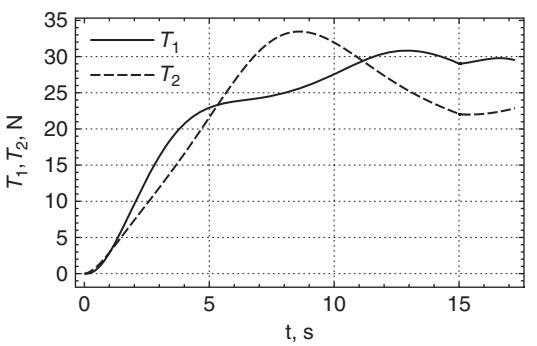

d) Tensions T_1, T_2

Fig. 9 Simulation results for case 2.

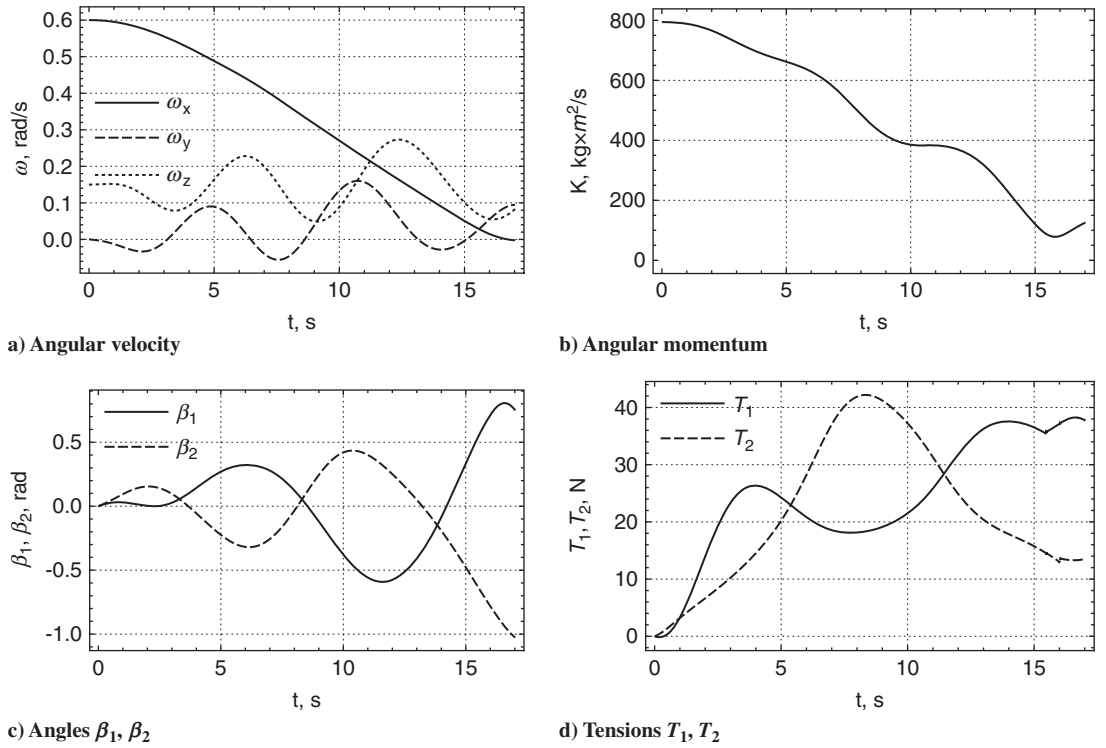

a) Angular velocity **b) Angular momentum**

c) Angles β_1, β_2 **d) Tensions T_1, T_2**

Fig. 10 Simulation results for case 3.

The simulation results are shown in Fig. 9. The angles α_1 and α_2 are changing over time in a similar way as in case 1, and the angular velocity ω_x decreases to zero within 17 s from the moment of releasing the masses (Fig. 9a). The angles β_1 and β_2 reach 0.3 rad due to the attitude motion of the target (Fig. 9c).

The angular momentum $|\boldsymbol{K}|$ does not reach zero due to the rotation of the target around the Cy and Cz axes. With the decreasing of the angular velocity ω_x, the angular momentum $J_x\omega_x$ decreases, but the sum of two other projections $J_y\omega_y$ and $J_z\omega_z$ remains almost unchanged, and so the nutation angle is increasing by the end of the despin process. It explains the increasing of angles β_1 and β_2. The tensions of the wires are different from each other and greater than zero throughout the whole despin process (Fig. 9d).

C. Case 3

In the third case, the angular velocity about Cz is 0.15 rad/s, and so the initial nutation angle is 11 deg. The simulation results are shown in Fig. 10. The angular velocity ω_x decreases to zero within 17 s as in the first two cases (Fig. 10a). The attitude motion of the debris excites high deflection of the wires from the plane of the reel. The angles between the Dy_dz_d plane and the wires exceed 1 rad (Fig. 10c). Figure 10d shows the time history of the wires' tension for case 3. We can see that the tension of the second wire is decreasing in the (8, 17) time interval but does not reach zero. Figure 10d illustrates asymmetry in the motion of the masses due to the spatial motion of the target.

The results illustrate that the angle between the plane of the reel and the wire exceeds 1 rad even if the initial nutation angle of the debris is as low as 11 deg. The simulation results suggest that the proposed scheme can be used to despin orbital stages that rotate mostly around their axis of symmetry. Spatial motion of the debris leads to a noticeable out-of-plane motion of the masses, which can lead to an unpredictable motion of the masses due to lack of the tensions of the wires.

V. Conclusions

The main contribution of this note is the scheme for despinning space debris using a modified yo-yo mechanism installed on the ADM module. The scheme can be used for space debris that rotates around the axis of symmetry with high angular velocity.

The modified yo-yo mechanism does not contribute to the space debris problem. Each mass of the mechanism consists of two separable dome-shaped shells filled with liquid. Instead of releasing the masses after despin, the liquid is released from the shell, for example, by separation of the mass into parts. Wire guides for the reel are proposed, which follow the motion of the wires and prevent coming off the wires from the reel due to the attitude motion of the debris.

A mathematical model of the spatial motion of the yo-yo mechanism is developed. The model is used to demonstrate the possibility of using the proposed scheme to despin space debris. The proposed scheme can be used to despin debris objects without using thruster engines. The rotation of the debris around the transverse axes also can be eliminated without using thrusters taking advantage of the tether connecting the tug with the ADM module. In this case, the design of the ADM module can be simplified.

Acknowledgment

This study was supported by the Russian Science Foundation (project number 16-19-10158).

References

[1] Liou, J.-C., and Johnson, N. L., "A Sensitivity Study of the Effectiveness of Active Debris Removal in LEO," *Acta Astronautica*, Vol. 64, Nos. 2–3, 2009, pp. 236–243. doi:10.1016/j.actaastro.2008.07.009

[2] Shan, M., Guo, J., and Gill, E., "Review and Comparison of Active Space Debris Capturing and Removal Methods," *Progress in Aerospace Sciences*, Vol. 80, Jan. 2016, pp. 18–32. doi:10.1016/j.paerosci.2015.11.001

[3] Bonnal, C., Ruault, J.-M., and Desjean, M.-C., "Active Debris Removal: Recent Progress and Current Trends," *Acta Astronautica*, Vol. 85, April–May 2013, pp. 51–60. doi:10.1016/j.actaastro.2012.11.009

[4] Schaub, H., and Sternovsky, Z., "Active Space Debris Charging for Contactless Electrostatic Disposal Maneuvers," *Advances in Space Research*, Vol. 53, No. 1, 2014, pp. 110–118. doi:10.1016/j.asr.2013.10.003

[5] Botta, E. M., Sharf, I., Misra, A. K., and Teichmann, M., "On the Simulation of Tether-Nets for Space Debris Capture with Vortex

Dynamics," *Acta Astronautica*, Vol. 123, June–July 2016, pp. 91–102. doi:10.1016/j.actaastro.2016.02.012

[6] Shah, S. V., Sharf, I., and Misra, A., "Reactionless Path Planning Strategies for Capture of Tumbling Objects in Space Using a Dual-Arm Robotic System," *AIAA Guidance, Navigation, and Control (GNC) Conference*, AIAA Paper 2013-4521, 2013, p. 18. doi:10.2514/6.2013-4521

[7] Gilardi, G., Kawamoto, S., and Kibe, S., "Capture of a Non-Cooperative Object Using a Two-Arm Manipulator," *Proceedings of the 55th International Astronautical Congress*, International Astronautical Congress Paper IAC-04-A.5.06, Paris, 2004. doi:10.2514/6.IAC-04-A.5.06

[8] Jasper, L. E. Z., Seubert, C. R., Schaub, H., Trushkyakov, V., and Yutkin, E., "Tethered Tug for Large Low Earth Orbit Debris Removal," *Advances in the Astronautical Sciences*, Vol. 143, Jan. 2012, pp. 2223–2242.

[9] Forward, R. L., Hoyt, R. P., and Uphoff, C. W., "Terminator Tether: A Spacecraft Deorbit Device," *Journal of Spacecraft and Rockets*, Vol. 37, No. 2, 2000, pp. 187–196. doi:10.2514/2.3565

[10] Aslanov, V. S., and Yudintsev, V. V., "Behaviour of Tethered Debris with Flexible Appendages," *Acta Astronautica*, Vol. 104, No. 1, 2014, pp. 91–98. doi:10.1016/j.actaastro.2014.07.028

[11] Aslanov, V. S., and Yudintsev, V. V., "Dynamics of Large Debris Connected to Space Tug by a Tether," *Journal of Guidance, Control, and Dynamics*, Vol. 36, No. 6, 2013, pp. 1654–1660. doi:10.2514/1.60976

[12] DeLuca, L., Bernelli, F., Maggi, F., Tadini, P., Pardini, C., Anselmo, L., Grassi, M., Pavarin, D., Francesconi, A., Branz, F., Chiesa, S., Viola, N., Bonnal, C., Trushlyakov, V., and Belokonov, I., "Active Space Debris Removal by a Hybrid Propulsion Module," *Acta Astronautica*, Vol. 91, Oct.–Nov. 2013, pp. 20–33. doi:10.1016/j.actaastro.2013.04.025

[13] Nishida, S.-I., and Kawamoto, S., "Strategy for Capturing of a Tumbling Space Debris," *Acta Astronautica*, Vol. 68, Nos. 1–2, 2011, pp. 113–120. doi:10.1016/j.actaastro.2010.06.045

[14] Kawamoto, S., Matsumoto, K., and Wakabayashi, S., "Ground Experiment of Mechanical Impulse Method for Uncontrollable Satellite Capturing," *Proceedings of the 6th International Symposium on Artificial Intelligence and Robotics & Automation in Space: i-SAIRAS 2001*, Canadian Space Agency, St-Hubert, QC, Canada, June 2001, pp. 1–0.

[15] Tsuda, Y., and Nakasuka, S., "New Attitude Motion Following Control Algorithm for Capturing Tumbling Object in Space," *Acta Astronautica*, Vol. 53, No. 11, 2003, pp. 847–861. doi:10.1016/S0094-5765(02)00213-8

[16] Tadini, P., Tancredi, U., Grassi, M., Anselmo, L., Pardini, C., Francesconi, A., Branz, F., Maggi, F., Lavagna, M., Deluca, L. T., Viola, N., Chiesa, S., Trushlyakov, V., and Shimada, T., "Active Debris Multi-Removal Mission Concept Based on Hybrid Propulsion," *Acta Astronautica*, Vol. 103, Oct.–Nov. 2014, pp. 26–35. doi:10.1016/j.actaastro.2014.06.027

[17] Moody, C. K., Probe, A. B., Masher, A., Woodbury, T., Saman, M., Davis, J., and Hurtado, J. E., "Laboratory Experiments for Orbital Debris Removal," *Proceedings of the AAS Guidance, Navigation, and Control Conference*, American Astronautical Soc., Springfield, VA, 2016, pp. 1–12.

[18] Fitz-Coy, N., and Chatterjee, A., "Spacecraft Detumbling Through Energy Dissipation," *Proceedings of the Flight Mechanics (Estimation Theory) Symposium*, Goddard Space Flight Center, Greenbelt, MD, 1992, pp. 23–37.

[19] Hovell, K., and Ulrich, S., "Attitude Stabilization of an Unknown and Spinning Target Spacecraft Using a Visco-Elastic Tether," *Proceedings of the 13th Symposium on Advanced Space Technologies in Robotics and Automation*, European Space Research & Technology Centre, Noordwijk, The Netherlands, 2015 (to be published).

[20] Cleary, S., and O'Connor, W. J., "Control of Space Debris Using an Elastic Tether and Wave-Based Control," *Journal of Guidance, Control, and Dynamics*, Vol. 39, No. 6, 2016, pp. 1392–1406. doi:10.2514/1.G001624

[21] O'Connor, M. J., Clearly, S., and Hayden, D., "Debris De-Tumbling and De-Orbiting by Elastic Tether and Wave-Based Control," *Proceedings of the 6th International Conference on Astrodynamics Tools and Techniques (ICATT)*, Darmstadt, Germany, 2016 (to be published).

[22] Aslanov, V. S., and Yudintsev, V. V., "Dynamics of Large Space Debris Removal Using Tethered Space Tug," *Acta Astronautica*, Vol. 91, Oct. Nov. 2013, pp. 149–156. doi:10.1016/j.actaastro.2013.05.020

[23] Jasper, L., and Schaub, H., "Discretized Input Shaping for a Large Thrust Tethered Debris Object," *Advances in the Astronautical Sciences*, Vol. 152, Univelt, Incorporated, San Diego, CA, Jan. 2014, pp. 3385–3403.

[24] Aslanov, V. S., and Yudintsev, V. V., "The Motion of Tethered Tug-Debris System with Fuel Residuals," *Advances in Space Research*, Vol. 56, No. 7, 2015, pp. 1493–1501. doi:10.1016/j.asr.2015.06.032

[25] Fedor, J. V., "Theory and Design Curves for a Yo-Yo De-Spin Mechanism for Satellites," NASA TR-D-1676, 1961.

[26] Fedor, J. V., "Analytical Theory of the Stretch Yo-Yo for De-Spin of Satellites," NASA TR-D-1902, 1963.

[27] Bement, L. J., and Schimmel, M. L., "Investigation of Super*Zip Separation Joint," NASA TR-D-4031, 1988.

[28] Choi, M., Lee, J.-R., and Kong, C.-W., "Development of a Numerical Model for an Expanding Tube with Linear Explosive Using AUTODYN," *Shock and Vibration*, Vol. 2014, March 2014, pp. 1–10. doi:10.1155/2014/436156

[29] Brandt, O. E., and Harris, J. G., "Explosive System," US3698281 A, 1972.

[30] Cornille, H. J., "A Method of Accurately Reducing the Spin Rate of a Rotating Spacecraft," NASA TR-D-1902, 1962, p. 3.

[31] Curtis, H., *Orbital Mechanics for Engineering Students*, Elsevier, Oxford, England, U.K., 2013.

[32] Schaub, H., and Junkins, J. L., *Analytical Mechanics of Space Systems*, AIAA Education Series, AIAA, Reston, VA, 2003, pp. 11, 34, 37, 112, 113. doi:10.2514/4.861550